Journal of Molecular Liquids 156 (2010) 45–51

Contents lists available at ScienceDirect

Journal of Molecular Liquids

journal homepage: www.elsevier.com/locate/molliq

Hydrodynamic size and scaling relations for linear and 4 arm star PVAc studied using PGSE NMR

Scott A. Willis, Gary R. Dennis, Gang Zheng, William S. Price *

Nanoscale Organisation and Dynamics Group, College of Health and Science, University of Western Sydney, Locked Bag 1797, Penrith South DC, NSW 1797, Australia

ARTICLE INFO

Available online 4 May 2010

Keywords:
Hydrodynamic radius
PGSE NMR
Self-diffusion
Star polymer

ABSTRACT

In this work the hydrodynamic radius and scaling relations of linear and 4 arm polyvinyl acetate (PVAc) were calculated from self-diffusion measurements. Self-diffusion coefficients at infinite dilution were estimated from measurements of self-diffusion at 25 °C in deuterated chloroform and in the dilute regime using pulsed gradient spin-echo (PGSE) nuclear magnetic resonance (NMR). Scaling laws were observed but unexpectedly these star polymers showed slightly larger hydrodynamic radii than the linear equivalents. Hydrodynamic radii were calculated for different Perrin or shape factors (i.e. spherical, cylindrical and ellipsoidal), and the equivalent hydrodynamic radii for the cylinders and ellipsoids were compared to those obtained for a spherical shaped molecule. These were also compared to an approximate equivalent hydrodynamic radius estimated using approximate dimensions of the polymers at maximum extension for the cylinder/ellipsoid molecular shapes. Results for cylinder and ellipsoid shapes were almost identical for the same aspect ratios as expected.

1. Introduction

Self-diffusion, the random translational movement of a particle without external force, is the most fundamental form of molecular transport. It is related to hydrodynamic properties such as molecular size/shape and intermolecular interactions. Translational diffusion studies can provide information about the solution properties of molecules. Pulsed gradient spin-echo (PGSE) is a versatile and non-invasive nuclear magnetic resonance (NMR) technique which can be used to measure self-diffusion [1]. The Stokes–Einstein–Sutherland equation relates the diffusion coefficient, D ($m^2\ s^{-1}$), of a particle to its hydrodynamic size, i.e. hydrodynamic radius, through the relationship of the diffusion coefficient, strictly the self-diffusion coefficient at infinite dilution, D^0, and the friction coefficient, f [1–5], by,

$$D^0 = \frac{k_B T}{f} = \frac{k_B T}{\chi \pi \eta R_H}, \tag{1}$$

where k_B is the Boltzmann constant, T is the temperature, f is the friction coefficient (J s m^{-2}) which for a solution depends on the viscosity of the solvent, η (Pa s), and also the shape of the diffusing species. f in Eq. (1) has been expanded for the simplest and crudest approximation of a spherical molecule [2,3] and other shapes will be described in Section 1.1. χ is a number that depends on if the diffusion is under 'stick' ($\chi = 6$) or 'slip' ($\chi = 4$) conditions, which characterises the interaction between the solute and the solvent, and typically the 'stick' condition is applicable for large solutes [6].

1.1. Hydrodynamic size and shape factors

To describe the molecular shape a shape factor, also referred to as the Perrin factor [7], is used [1]. The shape factor, F_{Shape}, is the ratio of friction coefficient of the molecular shape, f, to that of a sphere, f^0, of equivalent volume, or is the ratio of the hydrodynamic radius of the shape, $R_{H,\text{ Shape}}$, to that of sphere of equivalent volume, $R_{H,\ eq}$ [7], that is [1,7,8],

$$F_{\text{Shape}} = \frac{f}{f^0} = \frac{R_{H,\text{ Shape}}}{R_{H,\ eq}}. \tag{2}$$

Note, for a spherical molecule $F_{\text{Sphere}} = 1$, since $f = f^0 = 6\pi\eta R_H$, where $R_H = R_{H,\ eq}$.

Other geometries are typically more suited to real molecules, for example cylinders or ellipsoids. One approximation, since exact analytical solutions are difficult to obtain [9], of the shape factor for a cylindrical molecule is [7],

$$F_{\text{Cylinder}} = 1.0304 + 1.93 \times 10^{-2}(\ln p) + 6.229 \times 10^{-2}(\ln p)^2 + 4.76 \times 10^{-3}(\ln p)^3 + 1.66 \times 10^{-3}(\ln p)^4 + 2.66 \times 10^{-6}(\ln p)^7, \tag{3}$$

* Corresponding author.
E-mail address: w.price@uws.edu.au (W.S. Price).

0167-7322/$ – see front matter © 2010 Elsevier B.V. All rights reserved.
doi:10.1016/j.molliq.2010.04.026

where $p = L/d$ is the aspect ratio and L is the length/height of the cylinder and d is its diameter, and this formula applies for the range of $p = 0.01$–100. Formulae for other ranges of p and other representations of this can be found in the literature [8–12].

A molecule shaped like a prolate ellipsoid has a shape factor of (e.g. see Ref. [7]),

$$F_{\text{Prolate Ellipsoid}} = \frac{\sqrt{p^2-1}}{p^{\frac{1}{3}}\ln\left[p+\sqrt{p^2-1}\right]}, \tag{4}$$

where $p = a/b$ is the aspect ratio, a is the polar radius of the ellipsoid and b is its equatorial radius. Note that for prolate ellipsoids $p>1$ since $a>b$. When $p<1$ the molecular shape is that of an oblate ellipsoid and the corresponding shape factor is (e.g. see Ref. [7]),

$$F_{\text{Oblate Ellipsoid}} = \frac{\sqrt{\left(\frac{1}{p}\right)^2-1}}{\left(\frac{1}{p}\right)^{\frac{2}{3}}\arctan\left(\sqrt{\left(\frac{1}{p}\right)^2-1}\right)}, \tag{5}$$

where p here is defined in the same way as for the prolate ellipsoid. Alternative representations of this can also be found in the literature [3,7,13].

When using Eqs. (3) and (4) it is useful to find $R_{H,\,eq}$ and compare it to that obtained for a spherical molecule, R_H, this can be achieved by using Eq. (1) and solving for $R_{H,\,eq}$,

$$R_{H,\,eq} = \frac{k_B T}{6\pi\eta D^0 F_{\text{Shape}}}. \tag{6}$$

1.2. Diffusion in dilute polymer solutions

Diffusion in polymer systems depends on the concentration for which the three regimes are dilute, semi-dilute and concentrated, and the boundary of dilute and semi-dilute is characterised by the critical overlap concentration, c^*, at which the polymers start to interact in solution [2,14–17]. A good estimate for this is $c^* = 1/[\eta]$ [18], where $[\eta]$ is the intrinsic viscosity of the polymer solution as given by the Mark–Houwink–Sakurada (MHS) equation, $[\eta] = KM^{\alpha}$ [2,19,20]. At concentrations less than c^* the solutions are termed dilute and the polymers are separated and interact only with solvent molecules [2]. For determination of the hydrodynamic radius the solutions studied need to be in the dilute regime and D^0 needs to be estimated, for this reason the concentration of the polymer solutions in this study were below c^*, which was estimated using $[\eta]$.

Scaling laws are commonly used to relate the physical properties such as the diffusion of a polymer to its molecular weight and/or concentration in solution [2,13,15,19–24]. The concentration dependence of D in dilute polymer solutions can be represented by [2,15,21,24],

$$D = D^0\left(1 + k_1 c + k_2 c^2 + \cdots\right), \tag{7}$$

where c is concentration and k_1, k_2 and others in the power series are constants that depend on the polymer and solvent. Typically the self-diffusion coefficient decreases linearly as c increases for low c [2] and can usually be satisfactorily fit to the first order expression of Eq. (7) [15,23,25].

For dilute solutions the proportionality of $D \propto M^{\nu}$ exists, where M is the molecular weight of the polymer [13,23,26]. This relationship depends on the polymer-solvent system [21,27–29] and ν can range from 0.5 (for a theta solvent, i.e. the polymer assumes unperturbed dimensions) −0.6 (for a good solvent, i.e. the polymers are expanded) [2,23,27–29], the values for this come from Flory theory and the Zimm model [2,13]. As branched polymers cannot be as extended in a good solvent as their linear equivalent, it is expected that $\nu<0.6$ [28]. However, these scaling laws may not account for changes in molecular shape, e.g. linear rods to random coils with increasing molecular weight [30]. The value of ν also reflects chain stiffness, D will be smaller for a rigid molecule when compared to a flexible one as it will be larger due to the rigid bonds [13], and so ν may be >0.6. Since D is proportional to hydrodynamic size through molecular weight, then scaling laws are expected for R_H [2,23,31,32]. The scaling laws typically observed are of the form,

$$R_H = kM^{\nu}, \tag{8}$$

where k is a scaling constant. Actually, the scaling relations are observed for the radius of gyration and the end to end distance, but since R_H is proportional to these then similar scaling is expected and similarly, scaling behaviour exists with respect to the number of monomers or statistical segments [2,13,15]. However, the exponent of the proportionality $R_H \propto M^{\nu}$ may be less than expected in some systems which may be due to partial draining conditions [32].

For polymer solutions, there are two extremes of frictional behaviour, these are free-draining and non-draining [1,20]. In the free-draining condition where the solvent molecules flow past each segment of the polymer as there are no hydrodynamic interactions, f in Eq. (1) is related to the number of segments and the friction per segment, with each segment having the same friction coefficient [1,20]. The more likely situation is the non-draining limit [1] or at least a combination of the free-draining and non-draining conditions [20]. In the non-draining condition the solvent molecules within the coil move with it, that is, there is strong hydrodynamic interaction, and the polymer coil can be modelled as an impermeable sphere. In this limit f is not directly proportional to number of segments in contrast to the free draining condition [1,20].

1.3. Aims

In this work we present the results of hydrodynamic radius calculations based on self-diffusion measurements on linear and 4 arm star polyvinyl acetate (PVAc) polymers using the PGSE NMR technique. Spherical, cylindrical (both rod and discs) and ellipsoid (both prolate and oblate) molecular shapes were considered and some brief considerations for the values of the aspect ratios, p, are given.

2. Experimental

2.1. Materials

Vinyl acetate (VAc, 99 + %) was purchased from Aldrich and was purified by passing it through an activated acidic alumina oxide (Aldrich, 150 mesh, 58 Å, surface area 155 $m^2\ g^{-1}$) column then distilled. Azodiisobutyronitrile (AIBN) was purchased from DuPont Pty Ltd, toluene (99.8%) from LabScan Analytical Sciences, tetrahydrofuran (THF, HPLC grade) from Ajax Finechem, narrow molecular weight polystyrene (PS) standards from Polymer Laboratories and except for the purified monomer and synthesised chain transfer agents, all were used as received. The standard methanol sample (99.97% MeOH + 0.03% HCl) for NMR temperature calibration was purchased from Wilmad. D_2O (99.9% D) and was purchased from Isotec Inc and $CDCl_3$ (99.8% D or 99.8%D with 1% TMS) was purchased from Cambridge Isotope Laboratories Inc. NMR tubes were Wilmad® NMR tubes (Wilmad Lab Glass, 5 mm, 528-PP). The linear chain transfer agent (methyl 2-(ethoxycarbonothioylthio) acetate, CTA_L) [33] and the four arm chain transfer agent (2,2-bis((2-(ethoxycarbonothioylthio)propanoyloxy)methyl)propane-1,3-diylbis(2

(ethoxycarbonothioylthio)propanoate), CTA_4) [34,35] were synthesized as described in literature.

2.2. Methods

2.2.1. Polymer synthesis and characterisation

Chain transfer agent (CTA_L or CTA_4), AIBN, VAc and toluene were transferred to ampoules and the solutions were thoroughly deoxygenated by three or four freeze – pump – thaw cycles under high vacuum after which the ampoules were flame-sealed. They were then placed in an oil bath at the required temperature and removed when necessary. The reactions were stopped by breaking the ampoule necks and evaporating the residual monomer and/or solvent on a steam bath.

Polymer molecular weights were determined via GPC analysis using a HP 1100 Series instrument. ChemStation for LC3D software (Agilent Technologies) was used for method and run control and ChemStation GPC data analysis software (Agilent Technologies) was used to analyse the data. Low resolution GPC was performed with a broad molecular weight column (Shodex® KF-806 M, 10 μm, exclusion limit: 2×10^7 g mol^{-1}) and high resolution GPC was performed with three PLgel, 5 μm, individual pore size columns (Polymer Laboratories; 10^3 Å [effective range: 500–60,000 g mol^{-1}], 10^4 Å [effective range: 10,000–600,000 g mol^{-1}] and 10^5 Å [effective range: 60,000–2,000,000 g mol^{-1}]). Polymers were eluted with THF at a flow rate of 1 mL min^{-1} with toluene flow marker. The GPC was calibrated with 10 narrow molecular weight PS standards and universal calibration was used to convert the PS equivalent weights of PVAc to the true PVAc weights. The MHS correction factors used for this were [19], $K=16\times10^{-3}$ mL g^{-1} and $\alpha=0.70$ (for PVAc) and $K=14\times10^{-3}$ mL g^{-1} and $\alpha=0.70$ (for PS). The PVAc polymers were purified via preparative GPC with a 10 mL min^{-1} flow rate through a guard column (PLgel Prep Guard, 25×25 mm, Polymer Laboratories) and a preparative column (PLgel, 10 μm, 10^3 Å, effective molecular weight range: 500–60,000 g mol^{-1}, Polymer Laboratories). High resolution GPC was then used to analyse the purified polymers. The peak molecular weight, M_p, and polydispersity index (PDI) of each polymer used for this study are given in Table 1.

2.2.2. PGSE NMR for diffusion measurements

^{1}H NMR diffusion experiments were performed at 25 °C with a Bruker Avance 400 MHz with 5 mm broadband X(H) probe equipped with a *z*-axis gradient. All data fitting for NMR calibration and diffusion measurement analysis, was performed using OriginPro 8 (OriginLab Corporation) software using the Levenberg–Marquardt algorithm. The temperature was calibrated using a standard methanol sample [36,37]. The gradient strength was calibrated by measuring the diffusion of the residual HOD in D_2O (400 μL) at 25 °C with the double stimulated echo (DSTE) [38] with trapezoidal gradient pulses (shown in Fig. 1). The maximum gradient strength was found to be 0.521 T m^{-1}.

Polymer diffusion measurements were also performed with this sequence, which was chosen to minimize convection problems and because in macromolecular samples the spin-lattice relaxation time, T_1, is much greater than the spin-spin relaxation time, T_2 [39]. The attenuation due to diffusion for this sequence with trapezoidal gradient pulses was derived for this study using Maple 12 (Maplesoft, Waterloo Maple, Inc.) and is given by,

$$E(g,\Delta) = \exp\left\{-\left[\gamma^2 g^2\left(\delta^2\left(\Delta-\frac{2\delta}{3}\right)+B_{\text{Trapezoid}}\right)\right]D\right\}$$

$$\text{where}\quad B_{\text{Trapezoid}} = \left(-2\delta\varepsilon\Delta+2\delta^2\varepsilon+\frac{16\varepsilon^3}{15}-\frac{35\delta\varepsilon^2}{15}+\varepsilon^2\Delta\right), \quad (9)$$

where γ is the gyromagnetic ratio of the nucleus, g is the gradient strength (T m^{-1}) and the delays (i.e. Δ, δ, τ_g, T, t_e, ε) (in s) are shown in Fig. 1. The attenuation is of the form described for the Stejskal and Tanner sequence with different gradient pulse shapes [39,40]. The data was normalized to the signal at 0.011 T m^{-1} gradient strength since the signal with 0 T m^{-1} gradient strength of stimulated echo type sequences can be affected by cosine modulation dependent on chemical shift [41,42]. Further experimental considerations can be found in the literature [1,39,41,43].

The diffusion coefficients for linear and 4 arm PVAc were measured in dilute 'monomodal' polymer solutions (i.e. only one M_p and one type of polymer present) at three concentrations, approximately 1.5% w/v, 0.75% w/v and 0.31% w/v. The PDI associated with each of these polymers was ignored for the analysis and the measured diffusion coefficients were assigned to a single molecular weight (i.e. M_p). Polymers were weighed directly into the NMR tubes and 400 μL of $CDCl_3$ was added and the tubes with lids were sealed with paraffin film. The polymer solutions were allowed to equilibrate for at least 3 h after which the solution was thoroughly stirred using a vortex mixer. The meniscus was marked to check for solvent evaporation during preparation and between NMR experiments.

Generally for the diffusion experiments, the values of δ, Δ, and g were selected so that the signal attenuated to 10% of the signal without gradient and then the attenuation was measured by varying g. Typically the recycle delay time between diffusion experiments was 28–35 s ($5\times T_1$ of $CHCl_3$, longer than any of the polymer resonances so that the diffusion coefficient of $CHCl_3$ could also be measured as a check), and depending on the polymer type, molecular weight and concentration, δ ranged from 2–8 ms, Δ ranged from 0.07–0.65 s, $\varepsilon=50$ μs, $\tau_g=200$ μs, $t_e=5$ ms, spectral width was 8250 Hz digitized into 8 k or 16 k data points, the gradient strength was typically varied from 0.011–0.469 T m^{-1} in increments of 0.029 T m^{-1} giving a total of 17 data points for each attenuation curve. Each spectrum was averaged over 8 scans. The CH signal, for linear and 4 arm PVAc, was integrated over the range 4.60–5.40 ppm. Non-linear regression with Eq. (9) was used to calculate the diffusion coefficients. D^0 was estimated by fitting the first order approximation of Eq. (7) to the results for each M_p. The hydrodynamic radii of the polymers were calculated using spherical, rod with $L>d$ and prolate ellipsoid with $p=3$, 6, 15 and 30, disc with $L<d$ and oblate ellipsoid with $p=0.01$,

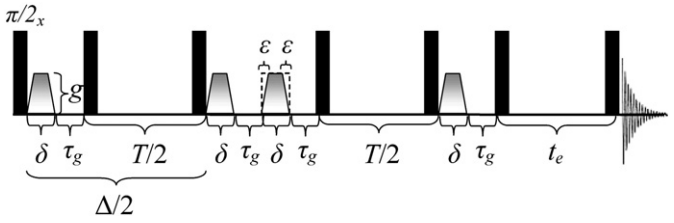

Fig. 1. The DSTE sequence with trapezoidal gradient pulses and a longitudinal eddy current delay (t_e) used in this work. This sequence is two stimulated echo (STE) type sequences joined with the diffusion time in each STE, $\Delta/2$, and the total diffusion time is Δ. The rise and fall time of the trapezoidal gradient pulses is ε and the total gradient pulse width is δ.

Table 1
Molecular weights and PDI of the synthesised PVAc polymers.

Linear PVAc		4 arm PVAc	
$M_p\times10^{-3}$ (g mol^{-1})	PDI	$M_p\times10^{-3}$ (g mol^{-1})	PDI
5	1.20	6.5	1.17
11	1.26	17	1.22
27	1.38	40	1.27
45	1.42	58	1.30
59	1.46	89	1.33
115	1.63	–	–

0.05, 0.2, 0.8 shape factors and using Eqs. (1)–(6) (where $\chi = 6$ and η ($CDCl_3$) $= 5.38611 \times 10^{-4}$ J s m^{-3} which is the corrected viscosity of $CHCl_3$ when deuterium is present using the viscosity ratio given by Holz [44]). The scaling laws with respect to the hydrodynamic radii and equivalent hydrodynamic radii for the cylinder and ellipsoid models were found (e.g. Eq. (8)) and compared to the estimated equivalent hydrodynamic radius for an extended polymer confined to the shape chosen (i.e. rod/disc or prolate/oblate ellipsoid). That is, a value of L and d for the rod and disc shapes and a value of a and b for the prolate and oblate ellipsoid shapes were crudely estimated from molecular dimension considerations. These are referred to here as L_{max} and d_{min} for a rod with $p>1$, L_{min} and d_{max} for a disc with $p<1$, a_{max} and b_{min} for a prolate ellipsoid, and a_{min} and b_{max} for an oblate ellipsoid but note that those with subscripts *min* may not strictly be the minimum. Using these, a molecular weight dependent aspect ratio, $p(M_p)$, was determined, as well as another equivalent hydrodynamic radius, $R_{H,\ eq\ A}$. $R_{H,\ eq\ A}$ was calculated by equating the volume of the cylinder to the volume of a sphere (e.g. Refs. [1,8]) and so,

$$R_{H,\ eq\ A} = L\left(3 \Big/ 16\left(p\left(M_p\right)\right)^2\right)^{\frac{1}{3}}, \tag{10}$$

where L here is L_{max} or L_{min} depending on if the shape is rods or discs. Similarly, equating the volume of the prolate or oblate ellipsoids to the volume of a sphere (e.g. Ref. [1]) and so,

$$R_{H,\ eq\ A} = \left(ab^2\right)^{\frac{1}{3}}, \tag{11}$$

where a and b here are a_{max} and b_{min} or a_{min} and b_{max} depending on if the shape is prolate or oblate ellipsoids. Note, the shape factor can also be considered dependent on molecular weight through the molecular weight dependent aspect ratio, $p(M_p)$. The errors taken for the diffusion coefficients, and hence the hydrodynamic radii, were the standard errors from the data fitting, but it should be noted that after including factors like inherent gradient inhomogeneity and gradient calibration errors one can expect a variation of order of 1% for duplicate measurements. The errors in the scaling laws are from the data fitting.

3. Results and discussion

As mentioned earlier, the PDI of the polymers was ignored for the analysis of the diffusion coefficients and the single molecular weight of M_p was assigned to the diffusion coefficients. The PGSE attenuations for the polymer solutions measured were mostly monoexponential and could be fit satisfactorily with Eq. (9) with fitting errors of <2%. A sample of the experimental attenuations and their corresponding fits are shown in Fig. 2. Actually, the polydispersity results in the measured diffusion coefficient being a weighted average, $\langle D\rangle_w$ [22,45], and so the hydrodynamic radius calculated using Eq. (1) will also be a weighted average, $\langle RH\rangle_w$. Hence, the hydrodynamic radii presented in this paper should be considered as weighted averages.

The hydrodynamic radius was first calculated with the spherical molecule model and the results are shown in Fig. 3. Interestingly the star PVAc was observed to diffuse slightly slower than the linear equivalent giving a slightly larger R_H and a higher scaling exponent, $\nu_{Star} = 0.58 \pm 0.01$ compared to $\nu_{Linear} = 0.53 \pm 0.01$. The full scaling laws are provided in the caption of Fig. 3. The deviation between the linear and star R_H increased with molecular weight, this is the same as a higher f for the star polymer. These results are in contrast to theoretical concepts that star polymers diffuse faster than their linear equivalent due to a more compact structure and limited expansion [2,46–49]. Actually other experimental results suggest that the reduction in the hydrodynamic radii aren't as large as what is expected from the theory and is attributed to the deviation from the requirement that the hydrodynamic shrinking factor assumes that the arms are undisturbed by the others giving a ratio of $R_{H,\ Star}/R_{H,\ Linear} < 1$ [47], but the ratio is still less than unity. The hydrodynamic shrinking factor may also vanish as molecular weight decreases because the expansion based on excluded volume increases [47]. Prats, Pla and Freire [46] acknowledged that both the theory and the synthetic techniques need improvement to allow for better comparison of the results for star polymers to the theory, as for example, uniform stars can be difficult to synthesise since there is the possibility that some arms grow more than others. At present we cannot provide a conclusive interpretation of the observed deviation from the theory but we speculate here that the core molecule used for the synthesis of the 4 arm PVAc may have an effect on these factors (i.e. the planar carbonyl and bulky methyl groups in the core may result in a higher expansion factor through rigidity and steric effects), alternatively the molecular shape may be different than from that of a 'spherical random coil' and the model of a spherical particle is oversimplified, the stars may have been non-ideal but still a branched polymer and also the polydispersity may have resulted in some sort of averaging of the hydrodynamic radii of the star and linear PVAc, as observed for diffusion coefficients [50].

The friction coefficient, f, was calculated using Eq. (1) with the assumption of a spherical molecule. The dependence of f on M_p is similar to that seen in Fig. 3 for the dependence of R_H on M_p. This is because f calculated in this way is simply a scaled version of R_H estimated using the spherical molecule model (i.e. $f = 6\pi\eta R_H$ as seen in Eq. (1)) and so is not shown as the graphs are identical except for the y-axes. Actually, the higher friction coefficient indicates a more expanded or rigid structure for the 4 arm star polymer.

The shape factor with the same p was considered for the linear and 4 arm star polymers separately, since applying the same shape factor to both simultaneously would shift both results to higher or lower $R_{H,\ eq}$. Recall that $R_{H,\ eq}$ here refers to the equivalent hydrodynamic radius based on a sphere of the same volume, see Section 1.1. Of course applying the same F_{Shape} for both architectures but with different p values results in differently displaced curves. The first shape factor considered was that of a rod shaped hydrodynamic particle, a cylindrical molecule with $p>1$ (i.e. Eq. (3)). The results are shown in Fig. 4 (applying F_{Cylinder} to the linear PVAc) and Fig. 5 (applying F_{Cylinder} to the 4 arm PVAc) and as expected the shape factor results in a lower $R_{H,\ eq}$ than R_H. Also as expected the scaling exponent (ν) for the scaling laws (i.e. Eq. (8)) shown in the captions of Figs. 4 and 5, are identical and only the scaling constant (k) shifts by the shape factor for a given p value. Consideration was given for the maximum allowed rod length (L_{max}) and a potential minimum diameter (d_{min}) to define one possible $p(M_p)$. For linear PVAc, L_{max} was taken as the fully extended length which is the contour length corrected for the bond angles along an all anti (or trans) configuration chain, $R_{c,\ all\ anti\ 'trans'\ config}$. While for the 4 arm PVAc, L_{max} was taken as twice the fully extended length of one arm which is twice the contour length of one arm corrected for the bond angles along an all anti configuration chain, $2R_{c,\ all\ anti\ 'trans'\ config\ per\ arm\ of\ star}$. Note that in the above calculations of L_{max}, the molecular weight of the core/end groups were not accounted for since the length is approximate in any case (i.e. due to PDI and assumptions). d_{min} is a little harder to define or estimate and was taken here as ~1 nm for the linear PVAc and ~2 nm for the 4 arm PVAc based on minimised energy 3D chemical models in Chem 3D Ultra (CambridgeSoft Corporation) and assumptions. $R_{H,\ eq\ A}$ was calculated using these values of L and d with Eq. (10). Lines corresponding to $R_{H,\ eq\ A}$ in Figs. 4 and 5 are effectively the lines defining when the volume of the hydrodynamic particle exceeds the volume of the extended and solvated polymer chain (or chains in the case of the star polymer). Since L_{max} depends on the molecular weight an M_p-dependent aspect ratio (i.e. $p(M_p)$) can be found. This could be used with the results for D^0 to find another equivalent hydrodynamic radius by, for example, using $p(M_p)$ in Eq. (3). For the definition of $p(M_p)$ using L_{max}, this would be $R_{H,\ eq}$ for a constant

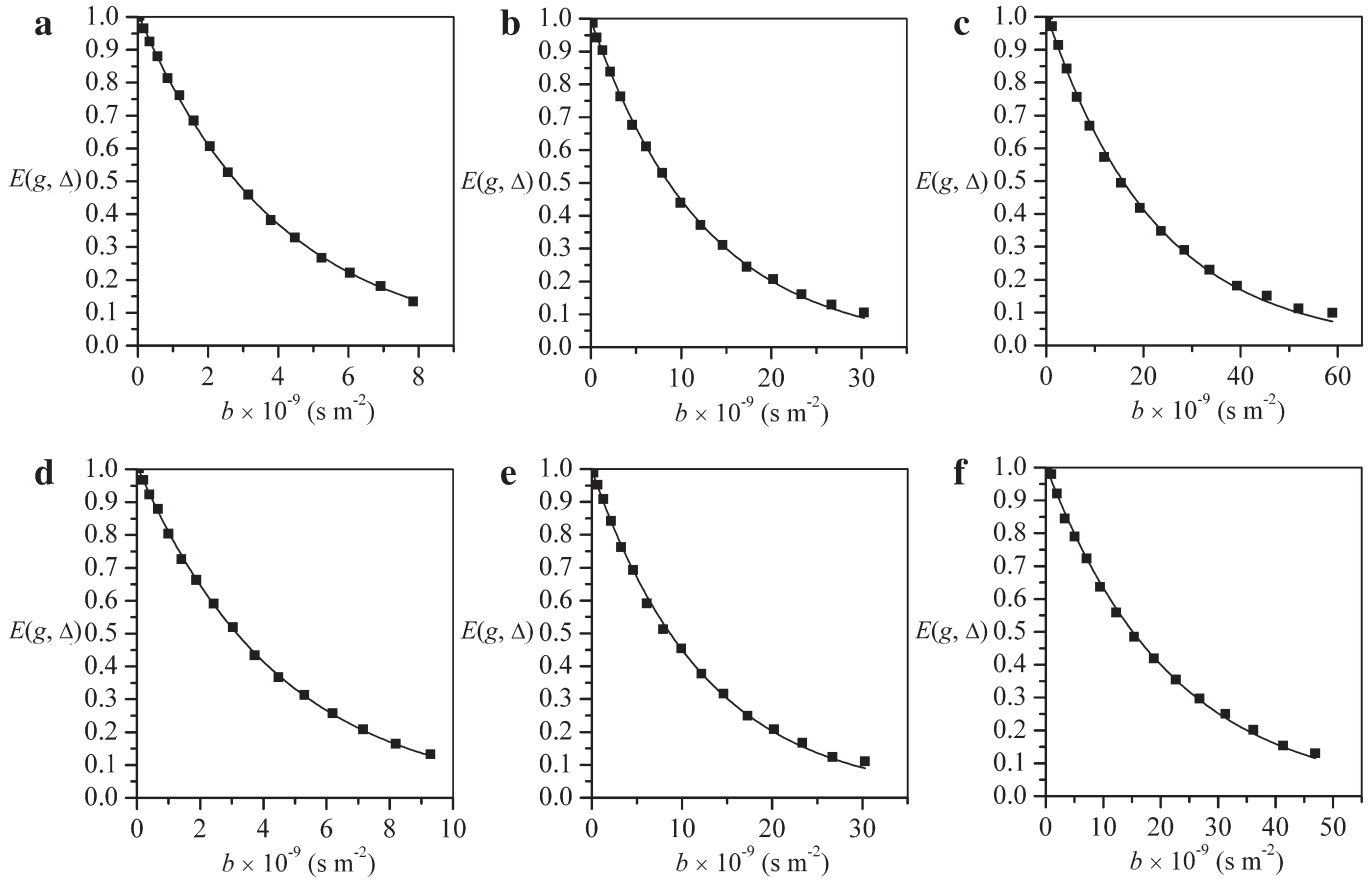

Fig. 2. Sample experimental attenuation curves and fits with Eq. (9) where $b=[\gamma^2 g^2(\delta^2(\Delta-2\delta/3)+B_{\text{Trapezoid}})]$. Linear PVAc: a. $M_p=5\times10^3$ g mol^{-1} and PDI = 1.20, b. $M_p=45\times10^3$ g mol^{-1} and PDI = 1.42, and c. $M_p=115\times10^3$ g mol^{-1} and PDI = 1.63. Four Arm PVAc: d. $M_p=6.5\times10^3$ g mol^{-1} and PDI = 1.17, e. $M_p=40\times10^3$ g mol^{-1} and PDI = 1.27, and f. $M_p=89\times10^3$ g mol^{-1} and PDI = 1.33. The samples shown have concentrations of 0.31% w/v.

d_{min}. However, $p(M_p)$ defined in this way is probably unrealistic as polymers are likely to adopt a random coil configuration in solution and so different dependencies of p on M_p would be more realistic. This could be useful to study systems where changes of p with M_p are known to occur. One example is low molecular weight DNA where the diameter may be constant but the length changes with increasing molecular weight as considered in Ref. [10].

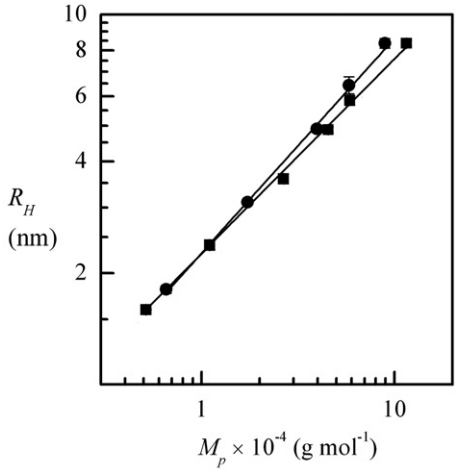

Fig. 3. R_H for a spherical molecule for the 4 arm star (●,—) and linear (■, —) PVAc calculated from Eq. (1) with $\chi=6$. The error bars are smaller than the symbols. The lines are fits to power laws (i.e. Eq. (8)) and for the 4 arm PVAc: $R_H=[(1.09\pm0.15)\times10^{-11}]M_p^{(0.58\pm0.01)}$ (m) and for the linear PVAc: $R_H=[(1.78\pm0.09)\times10^{-11}]M_p^{(0.53\pm0.01)}$ (m).

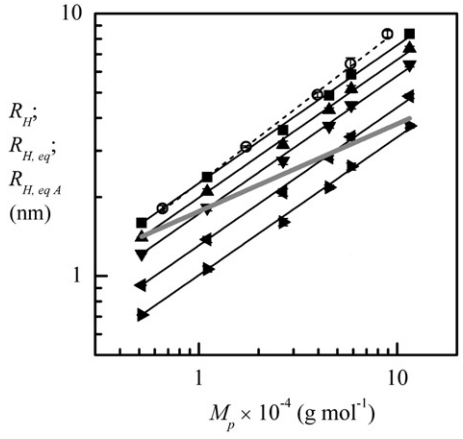

Fig. 4. Hydrodynamic radius calculations for linear PVAc (solid symbols and lines) using a rod shape molecule and comparisons to the results from the spherical molecule assumption and equivalent hydrodynamic radius from $p(M_p)$. R_H for a spherical molecule for the 4 arm star (○, - - -) and the linear (■, —) PVAc. $R_{H,\,eq}$ for the rod molecular shape ($p>1$) for the linear PVAc for $p=3$ (▲, —), $p=6$ (▼, —), $p=15$ (◄, —) and $p=30$ (►, —). Calculation using $p(M_p)$ assuming $L_{max}=R_{c,\,all\ anti\ 'trans'\ config}$ and that the $d_{min}\sim1$ nm (very crude) of $R_{H,\,eq\ A}$ for linear PVAc (▬) is from the formula for equivalent volume using the L_{max} and d_{min} values. The error bars are mostly smaller than the symbols, and all except the calculated $R_{H,\,eq\ A}$ have error bars. The lines are fits to power laws (but note that the definition of $R_{H,\,eq\ A}$ means it will have exponent of 1/3), these are 4 arm PVAc and linear PVAc spherical particles: as before in Fig. 3, linear PVAc rod with $p=3$: $R_{H,\,eq}=[(1.57\pm0.08)\times10^{-11}]M_p^{(0.53\pm0.01)}$ (m), $p=6$: $R_{H,\,eq}=[(1.36\pm0.07)\times10^{-11}]M_p^{(0.53\pm0.01)}$ (m), $p=15$: $R_{H,\,eq}=[(1.03\pm0.05)\times10^{-11}]M_p^{(0.53\pm0.01)}$ (m), $p=30$: $R_{H,\,eq}=[(7.96\pm0.40)\times10^{-12}]M_p^{(0.53\pm0.01)}$ (m), linear PVAc rod $R_{H,\,eq\,A}$: $R_{H,\,eq\,A}=[8.18\times10^{-11}]M_p^{(0.33)}$ (m).

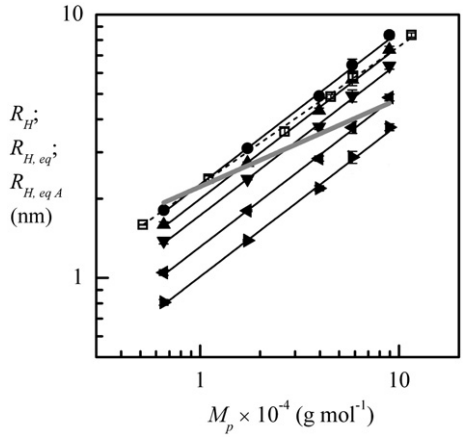

Fig. 5. Hydrodynamic radius calculations for the 4 arm star PVAc (solid symbols and lines) using a rod shape molecule and comparisons to the results from the spherical molecule assumption and equivalent hydrodynamic radius from $p(M_p)$. R_H for a spherical molecule for the 4 arm star (●, —) and linear (□, - - -) PVAc. $R_{H,\,eq}$ for the rod molecular shape ($p>1$) for the 4 arm PVAc for $p=3$ (▲, —), $p=6$ (▼, —), $p=15$ (◄, —) and $p=30$ (►, —). Calculation using $p(M_p)$ assuming $L_{max}=2R_{c,\,all\ anti\ 'trans'\ config\ per\ arm\ of\ star}$ and that the d_{min} ~2 nm (very crude) of $R_{H,\,eq\,A}$ for 4 arm PVAc (▬) is from the formula for equivalent volume using the L_{max} and d_{min} values. The error bars are mostly smaller than the symbols, and all except the calculated $R_{H,\,eq\,A}$ have error bars. The lines are fits to power laws (but note that the definition of $R_{H,\,eq\,A}$ means it will have exponent of 1/3), these are 4 arm PVAc and linear PVAc spherical particles: as before in Fig. 3 and 4 arm PVAc rod with $p=3$: $R_{H,\,eq}=[(9.57\pm1.36)\times10^{-12}]M_p^{(0.58\pm0.01)}$ (m), $p=6$: $R_{H,\,eq}=[(8.30\pm1.18)\times10^{-12}]M_p^{(0.58\pm0.01)}$ (m), $p=15$: $R_{H,\,eq}=[(6.29\pm0.90)\times10^{-12}]M_p^{(0.58\pm0.01)}$ (m), and $p=30$: $R_{H,\,eq}=[(4.85\pm0.69)\times10^{-12}]M_p^{(0.58\pm0.01)}$ (m), 4 arm PVAc rod for $R_{H,\,eq\,A}$: $[(1.03\times10^{-10}]M_p^{(0.33)}$ (m).

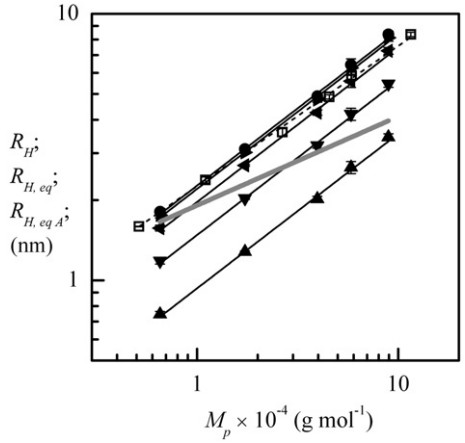

Fig. 7. Hydrodynamic radius calculations for the 4 arm star PVAc (solid symbols and lines) using a disc shape molecule and comparisons to the results from the spherical molecule assumption and equivalent hydrodynamic radius from $p(M_p)$. R_H for a spherical molecule for the 4 arm star (●, —) and linear (□, - - -) PVAc. $R_{H,\,eq}$ for the disc molecular shape ($p<1$) for the 4 arm PVAc for $p=0.01$ (▲, —), $p=0.05$ (▼, —), $p=0.2$ (◄, —) and $p=0.8$ (►, —). Calculation using $p(M_p)$ assuming L_{min} ~1 nm and that the $d_{max}=\sqrt{16R_{c,\,all\ anti\ 'trans'\ config\ per\ arm}L_{min}/\pi}$ (very crude) of $R_{H,\,eq\,A}$ for 4 arm PVAc (▬) is from the formula for equivalent volume using the L_{min} and d_{max} values. The error bars are mostly smaller than the symbols, and all except the calculated $R_{H,\,eq\,A}$ have error bars. The lines are fits to power laws (but note that the definition of $R_{H,\,eq\,A}$ means it will have exponent of 1/3), these are 4 arm PVAc and linear PVAc spherical particles: as before in Figs. 3 and 4 arm PVAc disc with $p=0.01$: $R_{H,\,eq}=[(4.48\pm0.64)\times10^{-12}]M_p^{(0.58\pm0.01)}$ (m), $p=0.05$: $R_{H,\,eq}=[(7.09\pm1.01)\times10^{-12}]M_p^{(0.58\pm0.01)}$ (m), $p=0.2$: $R_{H,\,eq}=[(9.43\pm1.34)\times10^{-12}]M_p^{(0.58\pm0.01)}$ (m), and $p=0.8$: $R_{H,\,eq}=[(1.06\pm0.15)\times10^{-11}]M_p^{(0.58\pm0.01)}$ (m), 4 arm PVAc disc for $R_{H,\,eq\,A}$: $[(8.87\times10^{-11}]M_p^{(0.33)}$ (m).

The next shape factor considered was that of a disc shaped hydrodynamic particle, a cylindrical molecule with $p<1$ (i.e. still Eq. (3)). The results are shown in Fig. 6 (applying F_{Cylinder} to the linear PVAc) and Fig. 7 (applying F_{Cylinder} to the 4 arm PVAc) and again the shape factor results in a lower $R_{H,\,eq}$ than R_H. Note again that it is only the scaling constant (k) that shifts due to the shape factor for a given

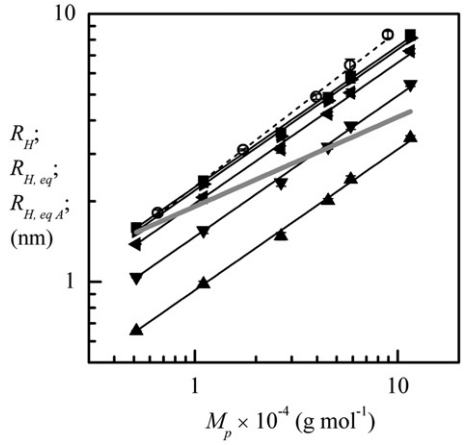

Fig. 6. Hydrodynamic radius calculations for linear PVAc (solid symbols and lines) using a disc shape molecule and comparisons to the results from the spherical molecule assumption and equivalent hydrodynamic radius from $p(M_p)$. R_H for a spherical molecule for the 4 arm star (○, - - -) and the linear (■, —) PVAc. $R_{H,\,eq}$ for the disc molecular shape ($p<1$) for the linear PVAc for $p=0.01$ (▲, —), $p=0.05$ (▼, —), $p=0.2$ (◄, —) and $p=0.8$ (►, —). Calculation using $p(M_p)$ assuming L_{min} ~1 nm and that the $d_{max}=\sqrt{4R_{c,\,all\ anti\ 'trans'\ config}L_{min}/\pi}$ (very crude) of $R_{H,\,eq\,A}$ for linear PVAc (▬) is from the formula for equivalent volume using the L_{min} and d_{max} values. The error bars are mostly smaller than the symbols, and all except the calculated $R_{H,\,eq\,A}$ have error bars. The lines are fits to power laws (but note that the definition of $R_{H,\,eq\,A}$ means it will have exponent of 1/3), these are 4 arm PVAc and linear PVAc spherical particles: as before in Fig. 3, linear PVAc disc with $p=0.01$: $R_{H,\,eq}=[(7.35\pm0.37)\times10^{-12}]M_p^{(0.53\pm0.01)}$ (m), $p=0.05$: $R_{H,\,eq}=[(1.16\pm0.06)\times10^{-11}]M_p^{(0.53\pm0.01)}$ (m), $p=0.2$: $R_{H,\,eq}=[(1.55\pm0.08)\times10^{-11}]M_p^{(0.53\pm0.01)}$ (m), $p=0.8$: $R_{H,\,eq}=[(1.73\pm0.09)\times10^{-11}]M_p^{(0.53\pm0.01)}$ (m), linear PVAc disc $R_{H,\,eq\,A}$: $R_{H,\,eq\,A}=[8.87\times10^{-11}]M_p^{(0.33)}$ (m).

p value. Consideration was given for the minimum allowed disc height (L_{min}) and a potential maximum diameter (d_{max}) to define one possible $p(M_p)$. For the case of disc molecular shapes the estimation of L_{min} and d_{max} are probably more crude than estimating the dimensions for rod molecular shapes. The following estimates are for the very crude assumption of a planar spiral for both the linear and 4 arm PVAc. For the case of the linear PVAc this is with one end of the long chain at the centre of the spiral and for the 4 arm PVAc this is with the core as the centre of the spiral. For both linear and 4 arm PVAc, L_{min} was crudely estimated as ~1 nm. d_{max} was taken as diameter of the spiral formed and is again related to the fully extended length for the linear PVAc and the fully extended length of one arm for the 4 arm PVAc. Note that in the above calculations of d_{max}, the molecular weight of the core/end groups were not accounted for since the length is approximate in any case (i.e. due to PDI and assumptions). $R_{H,\,eq\,A}$ was calculated using these values of L and d with Eq. (10). Lines corresponding to $R_{H,\,eq\,A}$ in Figs. 6 and 7 are effectively the lines defining when the volume of the hydrodynamic particle exceeds the volume of the spiral formed from the extended and solvated polymer chain (or chains in the case of the star polymer). Again, as d_{max} depends on the molecular weight an M_p-dependent aspect ratio (i.e. $p(M_p)$) can be found. This could be used with the results for D^0 to find another equivalent hydrodynamic radius by, for example, using $p(M_p)$ in Eq. (3). For the definition of $p(M_p)$ using d_{max}, this would be $R_{H,\,eq}$ for a constant L_{min}. Again, $p(M_p)$ defined in this way is probably unrealistic as polymers are likely to adopt a random coil configuration in solution and so different dependencies of p on M_p would be more realistic. As mentioned previously, this could be useful to study systems where changes of p with M_p are known to occur.

Prolate and oblate ellipsoid models were also considered using Eqs. (4) and (5). These showed very similar results to those of the cylindrical model with $p>1$ (rod) and $p<1$ (disc) and so the results are not shown here. This similarity is expected from the similar shape factors in the range of p used (see Fig. 8). However, the results for the oblate ellipsoid model differed more from the disc model than the prolate ellipsoid model did from the rod model. This can be seen in

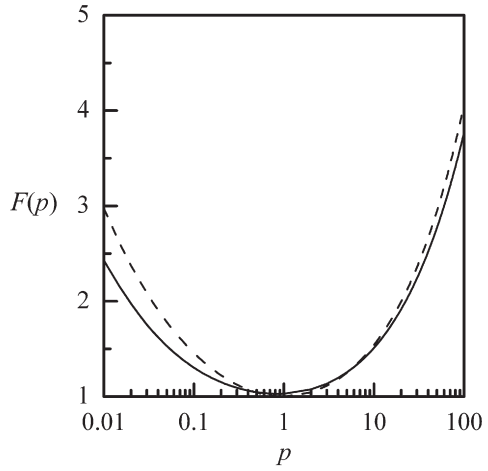

Fig. 8. The shape factors for ellipsoid (- - -) and cylindrical (—) shaped molecules in the range of $p = 0.01–100$. These were simulated using Eqs. (3)–(5). Prolate ellipsoids and rods have the range of $p>1$, while oblate ellipsoids and discs have the range of $p<1$.

Fig. 8 as the deviation of the oblate and disc shape factors for decreasing p. The oblate ellipsoid model resulted in lower values of $R_{H,\,eq}$ than the disc model since the shape factor was less for the disc model at lower p values.

Similar consideration was given for the maximum and minimum allowed value of the polar radius, a_{max} and a_{min}, and potential minimum and maximum value of the equatorial radius, b_{min} and b_{max}, as was done for the cylinder model with L and d. For prolate ellipsoids and for linear PVAc, a_{max} was taken as half the fully extended length, $L_{max}/2$ where L_{max} is that defined for the rod molecule of the linear PVAc. While for the 4 arm PVAc, a_{max} was taken as the fully extended length of one arm, $L_{max}/2$ where L_{max} is that defined for the rod molecule of the 4 arm PVAc. Again, b_{min} was a little harder to define or estimate and was taken here as ~0.5 nm for the linear PVAc and ~1 nm for the 4 arm PVAc. Note that defining a_{max} and b_{min} in this way is expected to give an ellipsoid that is too small compared to the rod model [9] which was observed for the line for $R_{H,\,eq\,A}$ (calculated from Eq. (11)) being at slightly lower values than the corresponding one for the rod molecule. A better choice for b_{min} is possibly $1.37(d_{min}/2)$ [9]. For oblate ellipsoids the crude approximation of planar spirals was again used, as was done for the disc shape. a_{min} was taken as $L_{min}/2$ and b_{max} was taken as equivalent to $d_{max}/2$ where L_{min} and d_{max} are those defined for the disc shaped molecules.

The shape factors chosen here were for simplicity, so that 'limits' of the aspect ratio could be assumed but other shapes, such as dumbbells or bent/hinged rods, may be better suited for calculating the hydrodynamic radius of a star polymer but are beyond the scope of the present paper. A discussion concerning other hydrodynamic models is given by García de la Torre and Bloomfield [9].

4. Conclusions

Hydrodynamic radii and scaling relations were found for synthesised linear and 4 arm star PVAc in deuterated chloroform at 25 °C. While the results showed typical scaling behaviour observed for polymer solutions it was noted that the star polymers had slightly higher hydrodynamic radii than the linear equivalents with increasing molecular weight when they were calculated using the spherical molecule assumption. Other Perrin factors were applied to the data for different aspect ratios, these were rods (cylinders with $p>1$), discs (cylinders with $p<1$), prolate and oblate ellipsoids. If the 4 arm star polymer had a different aspect ratio and/or shape factor compared to the linear equivalent then the calculated equivalent hydrodynamic radii may be less than that of the linear, of course the opposite could also be the case. The results for the cylinder and ellipsoid shapes were identical as expected from the similarity of the shape factors for the same aspect ratios. Simple (and crude) molecular weight dependent aspect ratios were considered and the line defined by these showed where the hydrodynamic volume exceeded the simplified molecular volume. The effects of polydispersity were not taken into account in the present study and a more complete consideration may include the effects of this as well as more realistic molecular shapes.

Acknowledgements

This research was supported by a University of Western Sydney Honours Scholarship (S.A.W.) and a N.S.W. BioFirst Award from the N.S.W. Ministry for Science & Medical Research (W.S.P.).

References

[1] W.S. Price, NMR Studies of Translational Motion, Cambridge University Press, New York, 2009.
[2] I. Teraoka, Polymer Solutions: An Introduction to Physical Properties, Wiley, New York, 2002.
[3] E.L. Cussler, Diffusion and Mass Transfer in Fluid Systems, Cambridge University Press, New York, 1997.
[4] W.S. Price, Concepts Magn. Reson. 9 (1997) 299.
[5] W. Sutherland, Philos. Mag. 9 (1905) 781.
[6] R. Ravi, D. Ben-Amotz, Chem. Phys. 183 (1994) 385.
[7] S. Hansen, J. Chem. Phys. 121 (2004) 9111.
[8] A. Ortega, J. García de la Torre, J. Chem. Phys. 119 (2003) 9914.
[9] J. García de la Torre, V.A. Bloomfield, Q. Rev. Biophys. 14 (1981) 81.
[10] M.M. Tirado, C.L. Martinez, J. García de la Torre, J. Chem. Phys. 81 (1984) 2047.
[11] M.M. Tirado, J. García de la Torre, J. Chem. Phys. 71 (1979) 2581.
[12] H. Yamakawa, G. Tanaka, J. Chem. Phys. 57 (1972) 1537.
[13] M. Doi, S.F. Edwards, The Theory of Polymer Dynamics, Oxford University Press, New York, 1986.
[14] Q. Ying, B. Chu, Macromolecules 20 (1987) 362.
[15] P.T. Callaghan, D.N. Pinder, Macromolecules 14 (1981) 1334.
[16] P.G. De Gennes, Macromolecules 9 (1976) 587.
[17] P.G. De Gennes, Macromolecules 9 (1976) 594.
[18] W. Brown, K. Mortensen, Macromolecules 21 (1988) 420.
[19] M. Kurata, Y. Tsunashima, Section VII–Solution Properties: Viscosity–Molecular Weight Relationships and Unperturbed Dimensions of Linear Chain Molecules, in: J. Brandrup, E.H. Immergut, E.A. Grulke, A. Abe, D.R. Bloch (Eds.), Polymer Handbook, Wiley, USA, 1999, VII/1–VII/68.
[20] R.J. Young, P.A. Lovell, Introduction to Polymers, Chapman & Hall, London, 1991.
[21] M.D. Lechner, E. Nordmeier, D.G. Steinmeier, Section VII—Solution Properties: Sedimentation Coefficients, Diffusion Coefficients, Partial Specific Volumes, Frictional Ratios, and Second Virial Coefficients of Polymers in Solution, in: J. Brandrup, E.H. Immergut, E.A. Grulke, A. Abe, D.R. Bloch (Eds.), Polymer Handbook, Wiley, USA, 1999, VII/85–VII/198.
[22] P.T. Callaghan, D.N. Pinder, Macromolecules 16 (1983) 968.
[23] T. Cosgrove, P.C. Griffiths, Polymer 36 (1995) 3335.
[24] P.T. Callaghan, Aust. J. Phys. 37 (1984) 359.
[25] A.I. Sagidullin, A.M. Muzafarov, M.A. Krykin, A.N. Ozerin, V.D. Skirda, G.M. Ignat'eva, Macromolecules 35 (2002) 9472.
[26] W. Hess, Macromolecules 20 (1987) 2587.
[27] R. Raghavan, T.L. Maver, F.D. Blum, Macromolecules 20 (1987) 814.
[28] R.A. Waggoner, F.D. Blum, J.C. Lang, Macromolecules 28 (1995) 2658.
[29] G. Vancso, Eur. Polym. J. 26 (1990) 345.
[30] A. Jerschow, N. Müller, Macromolecules 31 (1998) 6573.
[31] B. Fritzinger, D. Appelhans, B. Voit, U. Scheler, Macromol. Rapid Commun. 26 (2005) 1647.
[32] K.F. Freed, S.Q. Wang, J. Roovers, J.F. Douglas, Macromolecules 21 (1988) 2219.
[33] M.H. Stenzel, L. Cummins, G.E. Roberts, T.P. Davis, P. Vana, C. Barner-Kowollik, Macromol. Chem. Phys. 204 (2003) 1160.
[34] J. Bernard, A. Favier, L. Zhang, A. Nilasaroya, T.P. Davis, C. Barner-Kowollik, M.H. Stenzel, Macromolecules 38 (2005) 5475.
[35] M.H. Stenzel, T.P. Davis, C. Barner-Kowollik, Chem. Commun. (2004) 1546.
[36] J. Cavanagh, W.J. Fairbrother, A.G. Palmer III, M. Rance, N.J. Skelton, Protein NMR Spectroscopy: Principles and Practice, Academic Press, Burlington, 2007.
[37] D.S. Raiford, C.L. Fisk, E.D. Becker, Anal. Chem. 51 (1979) 2050.
[38] A. Jerschow, N. Müller, J. Magn. Reson. 125 (1997) 372.
[39] W.S. Price, Concepts Magn. Reson. 10 (1998) 197.
[40] W.S. Price, P.W. Kuchel, J. Magn. Reson. 94 (1991) 133.
[41] C.S. Johnson Jr, Prog. Nucl. Magn. Reson. Spectrosc. 34 (1999) 203.
[42] A. Chen, C.S. Johnson, M. Lin, M.J. Shapiro, J. Am. Chem. Soc. 120 (1998) 9094.
[43] W.S. Price, P. Stilbs, B. Jonsson, O. Soderman, J. Magn. Reson. 150 (2001) 49.
[44] M. Holz, X.-a. Mao, D. Seiferling, A. Sacco, J. Chem. Phys. 104 (1996) 669.
[45] W.S. Price, F. Tsuchiya, Y. Arata, J. Am. Chem. Soc. 121 (1999) 11503.
[46] R. Prats, J. Pla, J.J. Freire, Macromolecules 16 (1983) 1701.
[47] K. Huber, W. Burchard, L.J. Fetters, Macromolecules 17 (1984) 541.
[48] F. Ganazzoli, M.A. Fontelos, G. Allegra, Polymer 34 (1993) 2615.
[49] B.J. Bauer, L.J. Fetters, W.W. Graessley, N. Hadjichristidis, G.F. Quack, Macromolecules 22 (1989) 2337.
[50] P.T. Callaghan, D.N. Pinder, Macromolecules 18 (1985) 373.